Optical Materials 31 (2009) 590–597

Contents lists available at ScienceDirect

Optical Materials

journal homepage: www.elsevier.com/locate/optmat

Orthorhombic nonlinear crystals of $Ag_xGa_xGe_{1-x}Se_2$ for the mid-infrared spectral range

Valeriy Badikov [a], Konstantin Mitin [b], Frank Noack [c], Vladimir Panyutin [a], Valentin Petrov [c,*], Alexander Seryogin [b], Galina Shevyrdyaeva [a]

[a] High Technologies Laboratory, Kuban State University, 149 Stavropolskaya Street, 350040 Krasnodar, Russia
[b] FSUE "SPA Astrophysica", 95 Volokolamskoe Chaussee, 125424 Moscow, Russia
[c] Max-Born-Institute for Nonlinear Optics and Ultrafast Spectroscopy, 2A Max-Born-Street, D-12489 Berlin, Germany

ARTICLE INFO

Article history:
Received 21 December 2007
Received in revised form 18 June 2008
Accepted 19 June 2008
Available online 6 September 2008

PACS:
42.70.Mp
42.65.Ky

ABSTRACT

We study the birefringence and nonlinearity of quaternary semiconductors of the type $AgGaGe_nSe_{2(n+1)}$, solid solutions in the system $AgGaSe_2$–$nGeSe_2$. The birefringence, e.g. $n_a - n_c$ at 1064.2 nm, increases from 0.114 for $n = 2$ ($AgGaGe_2Se_6$) to 0.149 for $n = 5$ ($AgGaGe_5Se_{12}$) which substantially exceeds the birefringence of the uniaxial $AgGaSe_2$ (~0.022), the parent compound in the limit $n = 0$. Sellmeier equations valid in the 0.6–11.5 μm range are constructed for the solid solutions with $n = 2...5$. All four quaternary compounds are optically negative biaxial crystals. The calculated second-harmonic generation (SHG) limit (minimum fundamental wavelength) is ≈1470 nm for $AgGaGe_2Se_6$ and ≈1240 nm for $AgGaGe_5Se_{12}$, for type-I interaction and propagation along the *Y* principal optical axis. These limits are much lower than the ≈3120 nm limit for type-I interaction in $AgGaSe_2$. Thus, the $AgGaGe_nSe_{2(n+1)}$ orthorhombic crystals can be used for SHG down to their band-edge. The results for the nonlinear coefficients of $AgGaGe_nSe_{2(n+1)}$ ($n = 3$, 4 and 5), obtained from phase-matched SHG, indicate weak dependence on the composition. On the average, the larger nonlinear coefficient d_{31} is very close to d_{36} of $AgGaSe_2$ (~30 pm/V) while d_{32} is roughly two times smaller.

1. Introduction

Several recent studies were devoted to the linear and nonlinear optical properties of the quaternary $Ag_xGa_xGe_{1-x}S_2$ or $AgGaGe_nS_{2(n+1)}$ (in the system $AgGaS_2$–$nGeS_2$) crystals with orthorhombic symmetry *mm2*, for n = 1...5. The results and all the literature that has appeared on this family of sulfide materials for nonlinear optics in the mid-IR can be found in a review book chapter which appeared in 2008 [1]. Much less attention has been paid to the selenide analogs of this series, although the first publication, including phase diagrams, covered both the $AgGaS_2$–$nGeS_2$ and $AgGaSe_2$–$nGeSe_2$ systems [2]. As can be expected for selenide compounds, the quaternary crystals of this type exhibit extended transparency in the mid-IR and higher nonlinearity in comparison to their sulfide counterparts. In the first publication, seven such compounds ($n = 1.5$, 1.75, 2, 3, 4, 5, 9) were characterized with respect to the lattice parameters, band-gap, melting temperature, and absorption coefficient and birefringence in the visible [2]. The range of such solid solutions was specified as $0.1 \leqslant x \leqslant 0.4$ where $x = 1/(n+1)$ or $n = (1-x)/x$. In fact, however, these compounds were discovered much earlier [3]. In this patent one finds also an upper transparency limit of 15 μm, a damage threshold of 30 MW/cm^2, and a nonlinear coefficient of ~34 pm/V for all selenides ($0.167 \leqslant x \leqslant 0.37$ or $n = 1.75$, 2, 3, 4, and 5). Some more information on the growth, band-gap and absorption edge of $Ag_{0.12}Ga_{0.12}Ge_{0.88}Se_2$ appeared later [4] while single crystals of $AgGaGe_3Se_8$ were shown to be transparent up to 16 μm [5].

Similar to the $Ag_xGa_xGe_{1-x}S_2$ series, in the case of $Ag_xGa_xGe_{1-x}Se_2$ the two compounds in the limits $x = 0$ and $x = 1$ are not isostructural. The solid solutions $Ag_xGa_xGe_{1-x}Se_2$ exist only in a limited range for the parameter x, and their properties are related to a much lesser extent to the properties of $AgGaSe_2$ and $GeSe_2$. While the chalcopyrite $AgGaSe_2$ with point group $\bar{4}2m$ has mature growth technology and is a well established and characterized nonlinear optical crystal, $GeSe_2$ exhibits several polymorphic forms. It can be assumed that the relevant phase of $GeSe_2$ is the centrosymmetric monoclinic one [6] with space group $C_{2h}^5 - P2_1/c$ (point group $2/m$) in analogy with the sulfide compounds [1,5,7]. The structure of the $Ag_xGa_xGe_{1-x}Se_2$ solid solutions results from the substitution of Ge^{4+} by Ga^{3+} in the $GeSe_2$ cation sublattice. The valence deficiency is compensated by Ag^+ ions filling the tetrahedral vacancies. On the basis of the structural studies, it can be assumed that the β-phase quaternary selenium

* Corresponding author.
E-mail address: petrov@mbi-berlin.de (V. Petrov).

0925-3467/$ - see front matter © 2008 Elsevier B.V. All rights reserved.
doi:10.1016/j.optmat.2008.06.015

compounds have the same C_{2v}^{19} space group (point group *mm2*) as the corresponding sulfides [2]. Note that the existence of the $AgGaGeSe_4$ compound (an analog of $AgGaGeS_4$), $x = 0.5$ or $n = 1$, although mentioned in previous literature, was not confirmed in these studies. The symmetry of polycrystalline $AgGaGeSe_4$ samples was indicated before to be tetragonal [8–10], and single crystals grown by chemical transport reaction showed indeed defect chalcopyrite structure [11].

The birefringence of the quaternary $Ag_xGa_xGe_{1-x}Se_2$ compounds increases with n, reaching a value of ≈0.43 for $n = 9$ near 700 nm [2], which provides a unique possibility for engineering the phase-matching capability. This property will be reconsidered here. If compared to other mixed crystals like $AgGa_xIn_{1-x}Se_2$ it should be outlined that with $Ag_xGa_xGe_{1-x}Se_2$ the desired uncritical phase-matching is achieved in combination with higher (relatively to $AgGaSe_2$) and not lower birefringence which results in an extended potential for applications at shorter wavelengths.

In fact, until now only one selenide compound, $AgGaGe_5Se_{12}$, has been thoroughly studied as a nonlinear crystal, on one hand estimating its nonlinear coefficients from phase-matched second-harmonic generation (SHG) and on the other hand demonstrating some advantages with respect to difference-frequency mixing to produce femtosecond pulses in the mid-IR [12]. The material was resistant to damage at least up to 80 GW/cm^2 for 50 fs pulses at 1400 nm. This stimulated further research on its growth and characterization: High scattering losses (of the order of 10 cm^{-1}) were observed in as grown crystals [13]. The nonlinear coefficients of $AgGaGe_3Se_8$ were also determined using phase-matched SHG [14]. It was shown that doping with Cu improves the transparency of the $Ag_xGa_xGe_{1-x}Se_2$ compounds in the visible and near-IR [15]. With 10 ns pulses at 1064 nm, damage was observed at 75 MW/cm^2 [15].

Here, we present a systematic study of the birefringence and the nonlinearity of the orthorhombic solid solutions $AgGaGe_nSe_{2(n+1)}$ focusing on four representatives, $n = 2\ldots5$. It is based on older measurements of the index of refraction, a refinement using phase-matched SHG to derive Sellmeier equations, and estimations of the nonlinear coefficients also from phase-matched SHG.

2. Dispersion, birefringence, and effective nonlinearity

As their sulfide counterparts, the quaternary $AgGaGe_nSe_{2(n+1)}$ compounds are grown by the Bridgman–Stockbarger method [2]. All measurements described in this work were performed on samples cut from single crystals grown at the High Technologies Laboratory, after annealing. The specified x-values correspond to the charge. Fig. 1 shows boules of grown $AgGaGe_5Se_{12}$.

Fig. 1. Photograph of single crystals of $AgGaGe_5Se_{12}$: The front boule has a size of $\phi = 18 \times 80$ mm.

Characteristic average rates for the growth of high optical quality $AgGaGe_nSe_{2(n+1)}$ crystals range from 2 to 8 mm/day for the different compounds. The present state of the art permits the growth of single crystals as large as 60–80 mm in length and 22 mm in diameter (Fig. 1) with an optical homogeneity of $\delta n < 1 \times 10^{-4}$ cm^{-1} achieved after post growth thermal annealing in a furnace for 30 days. The homogeneity of the crystals, both along the growth and in the radial directions, was tested by monitoring the orientation of the two optic axes *C1* and *C2* in dependence on the position. Oriented wedged plates with a diameter of 1–2 cm and an angle between the normal and the *C1* or *C2* axis of 10°–15° were scanned across their surface with a step of 4–5 mm using a spot size of about 2 mm. This angle was found to be constant within the accuracy of the measurement (10′–20′) which leads to a maximum variation of the x parameter of the order of 0.002.

Table 1 summarizes some important properties of the studied compounds. The lattice constants are from the first publication [2]; other data appeared in the literature only on $AgGaGe_3Se_8$ [7]. It can be seen that with increasing n the two optic axes *C1* and *C2* move from the *ca* crystallographic plane to the *cb* plane. Note that per definition they lie in the *XZ* principal optical plane. The values for the angle between these axes and the *X* principal optical axis in the table are from the present work. The calculated angles are very close to the measured ones at 633 nm, see Fig. 2a. All four compounds are optically negative biaxial crystals, compare Table 1 and Fig. 2b.

The starting point for fitting of two-pole Sellmeier equations were the measured in the beginning of the 1980s [16], but unfortunately unpublished refractive indices from 0.6 to 11.5 μm, included in Table 2. The same table shows the values calculated by the derived here Sellmeier equations as well as the differences $\Delta n = n_{exp} - n_{calc}$ for the three refractive indices n_a, n_b, and n_c. Note that according to the conventions $n_X \leqslant n_Y \leqslant n_Z$.

For refinement of the Sellmeier equations, we used the measured angles between the two optic axes (see Fig. 2a) and (only for $n = 3$, 4, and 5) SHG data obtained from two different experimental set-ups. The first system was based on optical parametric amplifiers (OPAs) pumped at 800 nm by a 1-kHz femtosecond Ti:sapphire regenerative amplifier. At 2.3 μm we used the idler output of a commercial β-BaB_2O_4 (BBO) based OPA (TOPAS, Light Conversion Ltd.). At longer wavelengths we used home-made OPAs which were seeded at the signal wavelength by the frequency-doubled idler output of the same BBO OPA. Depending on the idler wavelength which ranged from 2.8 to 4.5 μm, either $KTiOPO_4$ (3 mm thick) or MgO:$LiNbO_3$ (2 mm thick) or $KNbO_3$ (4 mm thick) were employed in the seeded OPA. In all cases the energy at the fundamental used in the SHG experiments amounted to several microjoules. The pulse duration ranged from 120 to 160 fs (increasing with the wavelength). At 10.6 μm (fundamental) we used a TEA CO_2 laser. It operated at 10 Hz in the TEM_{00} mode and provided 120 ns long pulses with energy of up to 100 mJ. For the SHG measurements, thin plates of 0.5 mm thickness were used, except at 10.6 μm where the thickness was ≈3 mm but the cut was the same.

The Sellmeier equations of the type $n^2 = A_1 + A_3/(\lambda^2 - A_2) + A_5/(\lambda^2 - A_4)$, where λ is in microns, are summarized for the four $AgGaGe_nSe_{2(n+1)}$ compounds ($n = 2$, 3, 4, and 5) in Table 3. Previously such equations were published only for $AgGaGe_5Se_{12}$ [12]; the coefficients in Table 3 for this case represent a refinement.

The refractive index $n_c = n_X$ is substantially smaller than n_a, n_b which are rather close but do not cross within the transparency range, except for $AgGaGe_3Se_8$. As already mentioned the increased birefringence, relative to one of the parent compounds $AgGaSe_2$, is

Table 1
Properties of the studied $AgGaGe_nSe_{2(n+1)}$ compounds for $n = 2$, 3, 4, and 5

Nonlinear crystal	$AgGaGe_2Se_6$	$AgGaGe_3Se_8$	$AgGaGe_4Se_{10}$	$AgGaGe_5Se_{12}$
Compound	$Ag_xGa_xGe_{1-x}Se_2$	$Ag_xGa_xGe_{1-x}Se_2$	$Ag_xGa_xGe_{1-x}Se_2$	$Ag_xGa_xGe_{1-x}Se_2$
	$x = 0.333$	$x = 0.25$	$x = 0.2$	$x = 0.1667$
Space (point) group symmetry	C_{2v}^{19} (mm2)	C_{2v}^{19} (mm2)	C_{2v}^{19} (mm2)	C_{2v}^{19} (mm2)
Lattice constants [Å]	$c = 7.06$	$c = 7.12$ (7.15)[7]	*c = 7.21*	$c = 7.26$
	$a = 12.53$	$a = 12.41$ (12.43)[7]	$a = 12.36$	$a = 12.32$
	$b = 23.91$	$b = 23.80$ (23.75)[7]	$b = 23.71$	$b = 23.64$
Cations/anions ratio in unit cell	8/12	7.5/12	7.2/12	7/12
Two-fold polar axis	*c*	*c*	*c*	*c*
Correspondence principal optical/crystallographic axes	*X*–*c*	*X*–*c*	*X*–*c*	*X*–*c*
	Y–*b*	*Y*–*b*	*Y*–*a*	*Y*–*a*
	Z–*a*	*Z*–*a*	*Z*–*b*	*Z*–*b*
Optic axes *C1*, *C2* plane and exp. (calc.) value of the angle V_c with the *c*-axis [°] at 633 nm	*XZ*(*ca*)	*XZ*(*ca*)	*XZ*(*cb*)	*XZ*(*cb*)
	23.4 (24.0)	11.5(11.6)	6.6 (6.6)	13.1 (13.4)

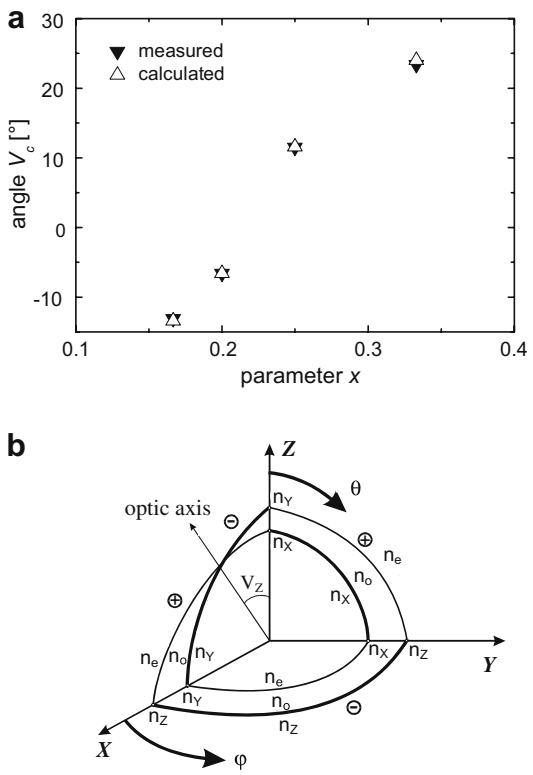

Fig. 2. (a) Measured angle V_c between the optic axes *C1*, *C2* and the *c*-axis of $Ag_xGa_xGe_{1-x}Se_2$ at 633 nm in dependence on the *x*-parameter (solid triangles) and calculated values (open triangles). The transition between the two crystallographic planes is illustrated assuming a different sign of this angle V_c. (b) Principal optical axes and types of interaction in a biaxial crystal. The two optic axes lie per definition in the *XZ* plane. V_Z is the angle they make with the *Z*-axis, $V_Z = 90^\circ - |V_c|$. For $n = 2,3$, $XYZ \equiv cba$ holds and for $n = 4,5$ $XYZ \equiv cab$ holds, see Table 1.

one of the main characteristic properties of the quaternary $AgGaGe_nSe_{2(n+1)}$ compounds. This is illustrated in Fig. 3a by plotting the difference between two of the refractive indices $n_a - n_c$. It can be seen that for all compounds the birefringence is much larger in comparison to $AgGaSe_2$. This means that much shorter wavelengths can be produced by SHG. The difference with $AgGaSe_2$ is due not only to the larger birefringence but also to the qualitatively different wavelength dependence of the birefringence which remains almost constant with wavelength while in $AgGaSe_2$ it exhibits an isotropic point near 813 nm.

The different correspondence between the crystallographic and principal optical axes leads to different expressions for the effective nonlinearity d_{eff}. In the principal planes it is given for $n = 4$ and 5 by:

$$d_{\text{eff}}(\text{oo-e}) = d_{32}\sin\varphi \quad \text{in the } XY \text{ plane} \tag{1}$$

$$d_{\text{eff}}(\text{ee-o}) = d_{32}\sin^2\theta + d_{31}\cos^2\theta \quad \text{in the } YZ \text{ plane} \tag{2}$$

$$d_{\text{eff}}(\text{oo-e}) = d_{31}\cos\theta \quad \text{in the } XZ \text{ plane } (\theta < 90^\circ - V_c) \tag{3}$$

For $n = 2$ and 3 these expressions defined in the *XYZ* frame remain unchanged due to the unchanged assignment $n_X = n_c$ which is related to the polar axis, however, the coefficients d_{31} and d_{32} have to be exchanged in them because for orthorhombic crystals they are traditionally defined in the *abc* frame. Thus, only type-I interaction is effective in these crystals. They behave like negative uniaxial in the *XY* and *XZ* planes and as positive uniaxial in the *YZ* plane. Since $d_{31} > d_{32}$ [12], most interesting for practical applications seems the engineerable by composition uncritical phase-matching along the *b*-axis. Fig. 3b shows the wavelength limits (fundamental) for uncritical SHG along the *a* and *b* crystallographic axes in dependence on the crystal composition. In both cases the interaction is of the oo-e type. As could be expected, the conventions adopted for the optical ellipsoid always lead to minimum SHG wavelength for propagation along the *Y* principal optical axis. Note that in all cases the generated second harmonic approaches the limits of the crystal transparency in the visible which are also expected to move to shorter wavelengths (larger band-gap) with decreasing value of the parameter *x* (increasing *n*) [2].

An interesting phenomenon can be observed in Fig. 3b for the compound $AgGaGe_3Se_8$ ($n = 3$ or $x = 0.25$). The minimum fundamental wavelengths for SHG along the *a* and *b* crystallographic axes differ by only ~0.4 nm. This composition corresponds to anomalous minimum in the dependence of the unit cell volume. The point corresponds to coinciding maxima of the solidus and liquidus curves in the phase diagram [5], which means that $AgGaGe_3Se_8$ can be regarded as a separate compound, with special position among the solid solutions in the $AgGaSe_2$–$n$$GeSe_2$ system. Therefore, even in the presence of slight deviations in the charge composition, it can be expected that this particular compound will grow with constant composition. It should be outlined that such a compound does not exist within the $AgGaS_2$–$n$$GeS_2$ system.

3. Nonlinear coefficients

The first estimation of the nonlinear coefficients of $AgGaGe_5Se_{12}$ was based on SHG using femtosecond pulses, as described earlier in relation to the refinement of the Sellmeier equations. Using samples of ~0.5 mm thickness, cut at $\theta = 61^\circ$ (*XZ* plane) and $\varphi = 18^\circ$ (*XY* plane) the result obtained at 3400 nm (fundamental) was: $d_{31} = 2.08d_{36}(AgGaS_2)$ and $d_{32} = 1.07d_{36}(AgGaS_2)$ [12]. For the present work we performed a number of such measurements for several wavelengths and three different compositions with ~0.5 mm thick samples cut in the *XZ* and *XY* planes.

Table 2
Measured (n_{exp}) and calculated (n_{calc}) refractive indices of $AgGaGe_nSe_{2(n+1)}$ compounds for $n = 2$, 3, 4, and 5

λ[nm]	$n_{c,exp}$	$n_{c,calc}$	Δn_c	$n_{a,exp}$	$n_{a,calc}$	Δn_a	$n_{b,exp}$	$n_{b,calc}$	Δn_b
$AgGaGe_2Se_6$, $n_X = n_c$, $n_Y = n_b$, $n_Z = n_a$									
600	2.674	2.674	0.000	2.832	2.832	0.000	2.800	2.800	0.000
700	2.593	2.593	0.000	2.727	2.728	−0.001	2.707	2.708	−0.001
800	2.549	2.549	0.000	2.674	2.674	0.000	2.657	2.658	−0.001
967	2.510	2.509	0.001	2.626	2.625	0.001	2.612	2.612	0.000
1064	2.496	2.495	0.001	2.609	2.609	0.000	2.597	2.596	0.001
2000	2.452	2.452	0.000	2.558	2.558	0.000	2.546	2.546	0.000
4000	2.439	2.439	0.000	2.543	2.543	0.000	2.531	2.530	0.001
8930	2.428	2.427	0.001	2.525	2.526	−0.001	2.511	2.511	0.000
10600	2.421	2.421	0.000	2.515	2.518	−0.003	2.502	2.502	0.000
11500	2.418	2.417	0.001	2.512	2.513	−0.001	2.497	2.497	0.000
$AgGaGe_3Se_8$, $n_X = n_c$, $n_Y = n_b$, $n_Z = n_a$									
600	2.626	2.627	−0.001	2.799	2.799	0.000	2.791	2.792	−0.001
700	2.550	2.550	0.000	2.707	2.705	0.002	2.699	2.699	0.000
800	2.509	2.509	0.000	2.652	2.654	−0.002	2.650	2.649	0.001
967	2.471	2.472	−0.001	2.605	2.606	−0.001	2.605	2.604	0.001
1064	2.458	2.460	−0.002	2.589	2.590	−0.001	2.589	2.588	0.001
2000	2.417	2.421	−0.003	2.539	2.539	0.000	2.539	2.540	−0.001
4000	2.404	2.409	−0.005	2.523	2.523	0.000	2.524	2.524	0.000
8930	2.395	2.395	0.000	2.508	2.505	0.003	2.505	2.504	0.001
10600	2.389	2.389	0.000	2.498	2.497	0.001	2.499	2.494	0.005
11500	2.385	2.384	0.001	2.491	2.492	−0.001	2.494	2.488	0.006
$AgGaGe_4Se_{10}$, $n_X = n_c$, $n_Y = n_a$, $n_Z = n_b$									
600	2.604	2.604	0.000	2.785	2.784	0.001	2.786	2.785	0.001
700	2.527	2.527	0.000	2.689	2.690	−0.001	2.694	2.694	0.000
800	2.487	2.487	0.000	2.639	2.639	0.000	2.645	2.645	0.000
967	2.451	2.451	0.000	2.593	2.593	0.000	2.600	2.600	0.000
1064	2.438	2.438	0.000	2.577	2.577	0.000	2.584	2.584	0.000
2000	2.397	2.400	−0.003	2.527	2.527	0.000	2.535	2.534	0.001
4000	2.384	2.388	−0.004	2.512	2.512	0.000	2.518	2.518	0.000
8930	2.374	2.374	0.000	2.496	2.495	0.001	2.501	2.499	0.002
10600	2.366	2.368	−0.002	2.484	2.487	−0.003	2.492	2.490	0.002
11500	2.362	2.363	−0.001	2.477	2.482	−0.005	2.482	2.484	−0.002
$AgGaGe_5Se_{12}$, $n_X = n_c$, $n_Y = n_a$, $n_Z = n_b$									
600	2.580	2.581	−0.001	2.773	2.771	0.002	2.784	2.783	0.001
700	2.508	2.507	0.001	2.680	2.682	−0.002	2.690	2.693	−0.003
800	2.469	2.468	0.001	2.629	2.632	−0.003	2.641	2.643	−0.002
967	2.433	2.433	0.000	2.584	2.586	−0.002	2.596	2.597	−0.001
1064	2.420	2.421	−0.001	2.568	2.571	−0.003	2.580	2.581	−0.001
2000	2.383	2.384	−0.001	2.521	2.520	0.001	2.532	2.530	0.002
4000	2.371	2.372	−0.001	2.506	2.505	0.001	2.517	2.514	0.003
8930	2.361	2.359	0.002	2.490	2.488	0.002	2.499	2.495	0.004
10600	2.358	2.352	0.006	2.480	2.480	0.000	2.490	2.486	0.004
11500	2.344	2.347	−0.003	2.475	2.475	0.000	2.480	2.480	0.000

Table 3
Sellmeier coefficients for the $AgGaGe_nSe_{2(n+1)}$ compounds ($n = 2$, 3, 4, and 5)

	n	A_1	A_2	A_3	A_4	A_5
$AgGaGe_2Se_6$ [0.6–11.5 μm]	n_X (n_c)	6.233430	0.1207668	0.2887427	519.06	151.5235
	n_Y (n_b)	7.563806	0.1188860	0.3477942	1044.74	1217.077
	n_Z (n_a)	7.381058	0.1383535	0.3458227	947.69	872.9966
$AgGaGe_3Se_8$ [0.6–11.5 μm]	n_X (n_c)	6.299683	0.1315100	0.2514435	698.27	349.5382
	n_Y (n_b)	8.358805	0.1279481	0.3301877	1535.63	3049.823
	n_Z (n_a)	7.327939	0.1188187	0.3569799	997.63	968.4704
$AgGaGe_4Se_{10}$ [0.6–11.5 μm]	n_X (n_c)	6.206128	0.1330557	0.2461451	707.91	359.0626
	n_Y (n_a)	7.437256	0.1251658	0.3402386	1162.24	1318.264
	n_Z (n_b)	8.112821	0.1182480	0.3424930	1502.93	2665.294
$AgGaGe_5Se_{12}$ [0.6–11.5 μm]	n_X (n_c)	6.053734	0.1286940	0.2397014	622.50	267.9402
	n_Y (n_a)	7.266163	0.1128978	0.3486195	1059.86	1059.400
	n_Z (n_b)	7.972008	0.1143643	0.3510133	1422.29	2354.520

In the small signal limit, the relative measurements were based on plane wave analysis with corrections only for the Fresnel losses and the index of refraction dependence of the SHG efficiency. No linear losses were taken into account for these thin samples. The dependence on the composition was within the experimental error. This situation is similar to the one observed with the sulfide compounds [1]. Hence, we estimated average values of the two nonlinear coefficients. The result (at a fundamental of 3500 nm) is $d_{31} = 1.9d_{36}(AgGaS_2)$ and $d_{32} = 0.78d_{36}(AgGaS_2)$ with relative errors of the order of 5%. Hence, $d_{31}/d_{32} = 2.4 \pm 0.2$. Using $d_{36}(AgGaS_2) = 13.15$ pm/V [17], a value transformed to 3500 nm using Miller's rule, one arrives at $d_{31} = 25$ pm/V and $d_{32} = 10.3$ pm/V.

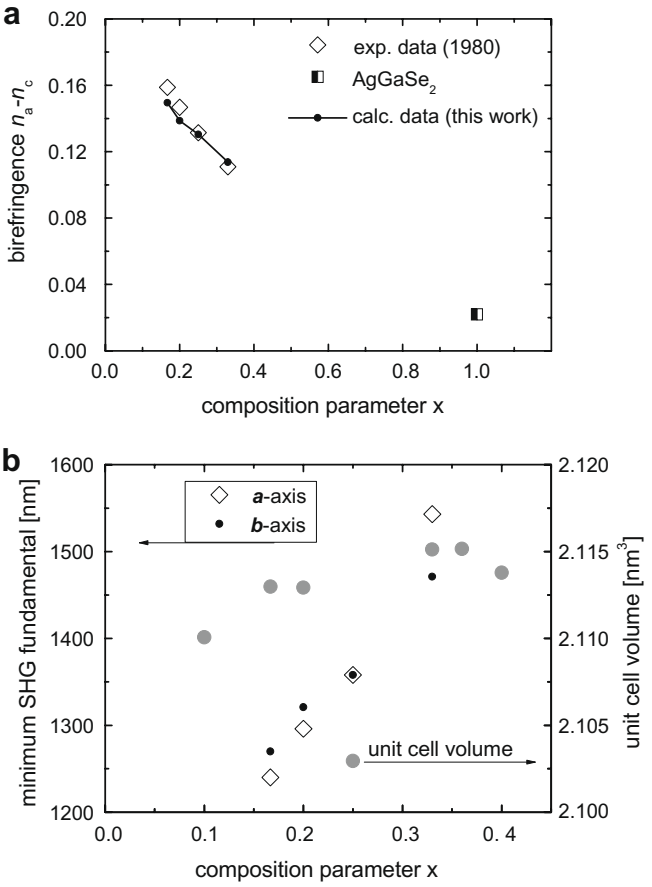

Fig. 3. (a) Birefringence of the biaxial $AgGaGe_nSe_{2(n+1)}$ compounds versus composition for $n = 2\ldots5$, in comparison to the birefringence of the uniaxial $AgGaSe_2$ (half full symbol) at 1064 nm. The open symbols represent the older measured data [3] while the solid symbols connected with a line are based on calculations using the constructed here two-pole Sellmeier expansions. (b) Minimum wavelengths (fundamental) for uncritical SHG along the *a* and *b* crystallographic axes of the $AgGaGe_nSe_{2(n+1)}$ compounds versus composition. The large grey circles show the evolution of the unit cell volume with the composition, calculated from the lattice parameters [2].

Thus d_{31} is roughly three times larger than the corresponding coefficient in the sulfide compounds [1].

The nonlinear coefficients of $AgGaGe_3Se_8$ were measured also by SHG at 10.6 μm, using the CO_2 laser described before and the same ~3 mm thick samples, under the same assumptions as with the femtosecond system. The reference sample of similar thickness was $AgGaSe_2$ in this case. The results of the measurements are shown in Fig. 4.

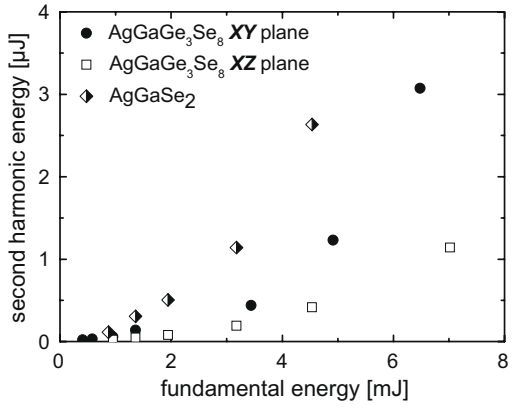

Fig. 4. Energy measured at the second harmonic (5.3 μm) versus incident energy at the fundamental (10.6 μm) for SHG in $AgGaGe_3Se_8$ (*XY* and *XZ* planes) in comparison to $AgGaSe_2$.

The analysis of the SHG data gave at this wavelength $d_{31} = (1.14 \pm 0.2)d_{36}(AgGaSe_2)$ and $d_{32} = (0.67 \pm 0.05)d_{36}(AgGaSe_2)$. The ratio $d_{31}/d_{32} = 1.7 \pm 0.3$ obtained here is much closer to the one observed in the sulfide compounds [1]. Having in mind the much closer second harmonic energies measured at 10.6 μm for the two $AgGaGe_3Se_8$ samples, it can be expected that this ratio and hence the value of the lower nonlinear coefficient are more reliable from the measurement using the CO_2 laser. Using $d_{36}(AgGaSe_2) = 29.3$ pm/V [18], a value corrected to 10.6 μm using Miller's rule, one arrives at $d_{31} = 33.4$ pm/V and $d_{32} = 19.6$ pm/V. Obviously, the difference in the larger nonlinear coefficient d_{31} is quite significant in the two SHG measurements. Note that this coefficient is more important for any applications because as we shall see the phase-matching properties in the two planes *XY* and *XZ* are quite similar. Unfortunately, the comparison of the two values is complicated by the great scatter in the data on the reference materials, although these are the two most established nonlinear crystals for the mid-IR spectral range. Thus, the value of $d_{36}(AgGaS_2)$ at 10.6 μm varies in the literature by almost a factor of 3 [19]. Hence, the same factor of uncertainty holds for the ratio $d_{36}(AgGaSe_2)/d_{36}(AgGaS_2)$. The only work where the nonlinear coefficient $d_{36}(AgGaSe_2)$ was measured relative to $d_{36}(AgGaS_2)$ gave a ratio of only 1.19 at 10.6 μm which is too low [20]. The values of $d_{36}(AgGaS_2)$ and $d_{36}(AgGaSe_2)$ that we used in the above evaluation of the nonlinear coefficients of the quaternary selenide compounds [17,18], give a ratio of 2.42 at 3500 nm and 2.66 at 10.6 μm. We tried to estimate this ratio using 0.5 mm thick plates for SHG at 3500 nm with the femtosecond system. The result, 2.09, was lower than the latter values but still much higher than obtained in the previous direct comparison [20]. With this in mind, the deviation of the d_{31} values obtained in the present work for the $AgGaGe_nSe_{2(n+1)}$ compounds by two different set-ups is within the experimental uncertainty.

4. SHG phase-matching characteristics

The most important feature of the SHG phase-matching curves calculated in Figs. 5 and 6 for $AgGaGe_5Se_{12}$ and in Figs. 7 and 8 for $AgGaGe_3Se_8$ (selected for its special position), is the nearly symmetric behavior in the *XY* and *XZ* planes due to the close values of the indices n_Y and n_Z. In the *YZ* plane where the tunability is very limited, the interaction is quasi-angle-noncritical which ensures large angular acceptance and small walk-off angle. This is much more pronounced for $AgGaGe_3Se_8$ as could be expected from the previous discussion. On the opposite, in the *XY* and *XZ* planes, there are regions of quasi-wavelength-noncritical phase-matching. The chosen presentation of the inverse group velocity mismatch, GVM, is equivalent to the spectral acceptance ($\Delta\nu L = 0.886/|\Delta_{31}|$) but contains the sign as additional information. Vanishing Δ_{31} means large spectral acceptance for SHG of short pulses where the second derivative of the wave-mismatch comes into play. The internal angular acceptance is calculated as FWHM in the small signal limit using analytical expressions analogous to those well-known for uniaxial crystals and critical phase-matching, i.e. only the first derivative of the wave-mismatch with respect to the angle is taken into account. The walk-off angle was calculated also using the simplified formalism valid for uniaxial crystals. Positive value of the walk-off angle means that the Poynting vector is at an angle larger than the phase-matching angle and vice versa. The three parameters $\rho_1, (=\rho_2), \rho_3$ designate the walk-off at the corresponding wave λ_1, ($=\lambda_2$), λ_3. Note, that in contrast to the older

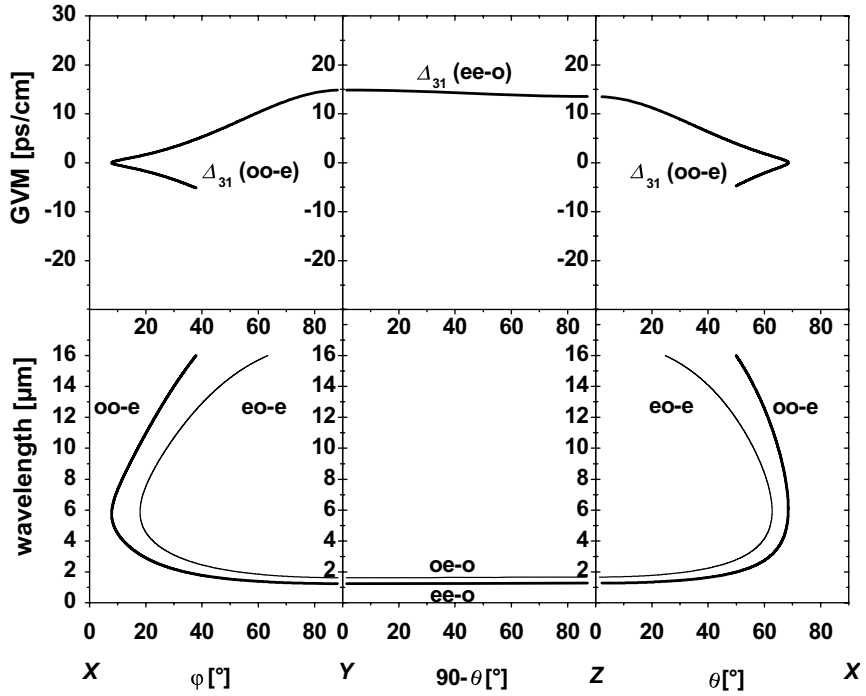

Fig. 5. SHG phase-matching in the principal planes of $AgGaGe_5Se_{12}$. Thick lines in the lower part show fundamental wavelengths for which $d_{eff} \neq 0$ and thin lines indicate cases where d_{eff} vanishes. The inverse group velocity mismatch, GVM ($\Delta_{31} = 1/v_3 - 1/v_1$ where v_1, (=v_2), v_3 denote the group velocities at λ_1, (=λ_2), and λ_3) is shown in the upper part only for the cases where $d_{eff} \neq 0$.

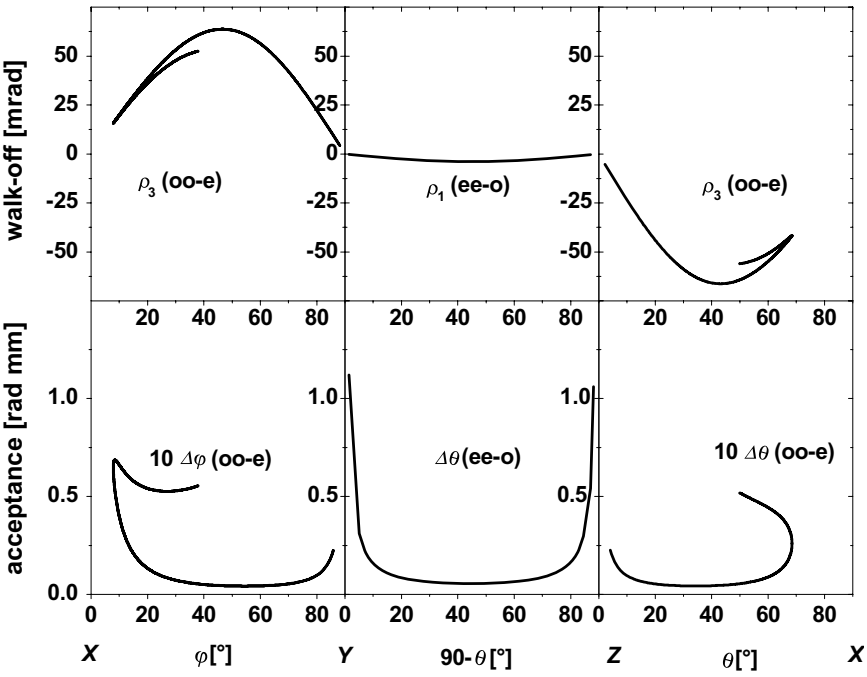

Fig. 6. SHG internal angular acceptance (bottom) and walk-off angles (top) in the principal planes of $AgGaGe_5Se_{12}$, for the cases when $d_{eff} \neq 0$.

Sellmeier equations for $AgGaGe_5Se_{12}$ [12], the new ones do not predict propagation along the *X*-axis.

The angular acceptance is calculated in Figs. 6 and 8 using only the linear approximation in the expansion of the wave-mismatch in order to preserve the scalability with the crystal thickness. This approximation is not valid in the vicinity of the principal optical axes and that is why the curves are interrupted in these regions. The effect is strongly pronounced in the case of $AgGaGe_3Se_8$ for the *YZ* plane (Fig. 8). In fact, the angular acceptance along the *Y* and *Z* axes of this crystal, calculated using the next, quadratic approximation but then for a given crystal thickness of say 1 cm, amounts to 1.13 rad, which coincides with the limits chosen for presenting Fig. 8. It is obvious that in this case more critical will be the angular acceptance in the other planes: Thus, using the second order approximation for a crystal thickness of 1 cm one obtains almost equal limiting angular acceptance of ~0.029 rad,

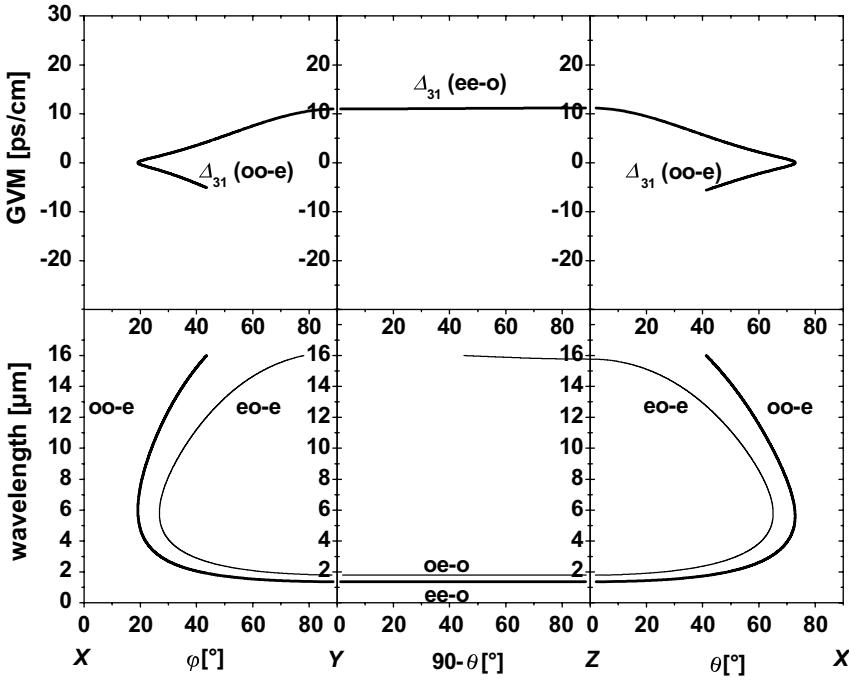

Fig. 7. SHG phase-matching in the principal planes of $AgGaGe_3Se_8$. Thick lines in the lower part show fundamental wavelengths for which $d_{eff} \neq 0$ and thin lines indicate cases where d_{eff} vanishes. The inverse group velocity mismatch, GVM ($\Delta_{31} = 1/v_3 - 1/v_1$ where v_1, (=v_2), v_3 denote the group velocities at λ_1, (=λ_2), and λ_3) is shown in the upper part only for the cases where $d_{eff} \neq 0$.

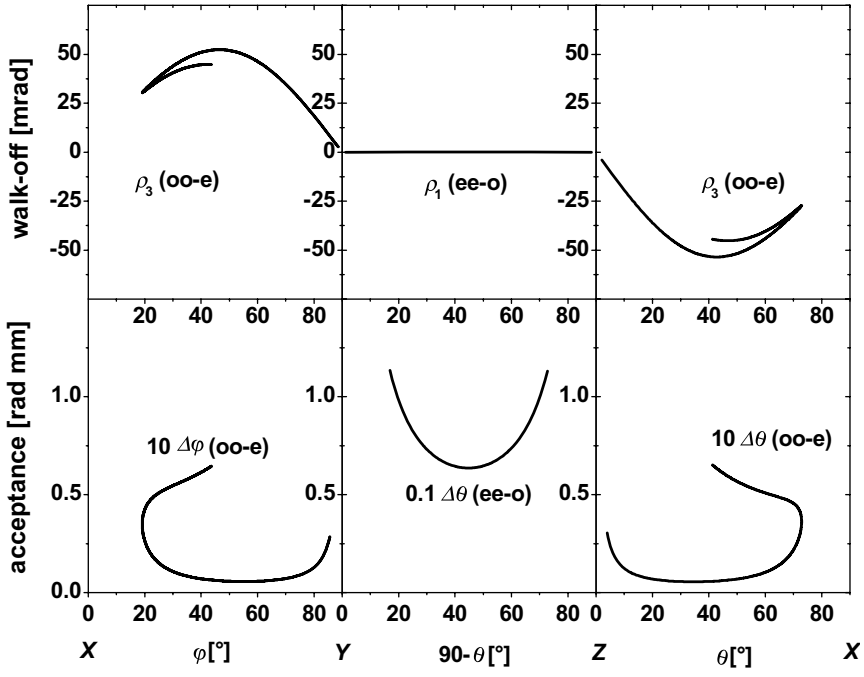

Fig. 8. SHG internal angular acceptance (bottom) and walk-off angles (top) in the principal planes of $AgGaGe_3Se_8$, for the cases when $d_{eff} \neq 0$.

both in the *XY* plane for propagation along the *Y* axis and in the *XZ* plane for propagation along the *Z* axis. This value is used as a limit for the corresponding curves in Fig. 8. Similarly, the limits of the acceptance angle curves in Fig. 6 correspond to the values for $AgGaGe_5Se_{12}$ along the *Y* and *Z* axes in the three respective principal planes, calculated using the second order derivatives for a crystal length of 1 cm.

One of the parent compounds, $AgGaSe_2$, is normally the crystal of choice for frequency doubling of 10.6 μm radiation. Unfortunately, for the $AgGaGe_nSe_{2(n+1)}$ compounds the phase-matching angles for this important application are not optimum and the effective nonlinearity is lower as can be concluded also from Fig. 4. Also the walk-off angle and the angular acceptance are roughly three times larger and smaller, respectively. Thus, the only potential advantage of these compounds with respect to SHG at 10.6 μm seems the expected higher damage threshold which is related to the larger band-gap but this still has to be experimentally confirmed. Other important characteristics of these crystals which

could be a subject of future research include the thermo-mechanical and thermo-optical properties.

5. Conclusion

In conclusion, we characterized the birefringence and the nonlinearity of the orthorhombic solid solutions $AgGaGe_nSe_{2(n+1)}$ for $n = 2...5$ using phase-matched SHG. Two-pole Sellmeier equations were constructed for these four quaternary compounds and SHG was then analyzed in terms of angle tuning, spectral and angular acceptance, and spatial walk-off in the three principal planes. We confirmed previous assumptions concerning the exceptionally large birefringence which enables SHG down to the absorption edge. The larger nonlinear coefficient of these crystals is independent of the exact composition and comparable to d_{36} of $AgGaSe_2$, one of the parent compounds. The compound $AgGaGe_3Se_8$ ($n = 3$) occupies a special position in this family of mid-IR crystals and deserves further attention especially in relation to its composition stability in the growth process.

Acknowledgment

This research leading to these results has received funding from the European Community's Seventh Framework Programme FP7/2007-2011 under grant agreement n° 224042.

References

[1] V. Petrov, V. Badikov, V. Panyutin, Quaternary nonlinear optical crystals for the mid-infrared spectral range from 5 to 12 micron, in: M. Ebrahimzadeh, I. Sorokina (Eds.), Mid-Infrared Coherent Sources and Applications, NATO Science for Peace and Security Series B: Physics and Biophysics, Springer, 2008, p. 105.
[2] V.V. Badikov, A.G. Tyulyupa, G.S. Shevyrdyaeva, S.G. Sheina, Inorg. Mater. 27 (1991) 177. Transl. from Izv. Akad. Nauk SSSR: Neorganicheskie Materialy 27(1991) 248.
[3] V.V. Badikov, E.A. Pobedimskaja, I.N. Matveev, N.K. Trotsenko, A.G. Tjuljupa, G.A. Shevyrdyaeva, L.N. Kaplunnik, "Non-linear single crystal material," Soviet Patent SU 1 839 800 A1 (C 30 B 29/46, 11.06), (application from 07.07.1980, published on 27.05.2005 Bull. 15). Note that the chemical formula given in the abstract is erroneous (S should read Se).
[4] I.D. Olekseyuk, G.E. Davidyuk, H.S. Bogdanyuk, A.P. Shavarova, V.V. Bozhko, G.P. Gorgut, A.F. Lomzin, Inorg. Mater. 29 (1993) 699. Transl. from Izv. Ross. Akad. Nauk: Neorganicheskie Materialy 29(1993) 617.
[5] I.D. Olekseyuk, A.V. Gulyak, L.V. Lisa, G.P. Gorgut, A.F. Lomzin, J. Alloys and Comp. 241 (1996) 187.
[6] G. Dittmar, H. Schäffer, Acta Cryst. B 32 (1976) 2726.
[7] I.D. Olekseyuk, G.P. Gorgut, O.V. Parasyuk, J. Alloys Comp. 260 (1997) 111.
[8] O.H. Hughes, J.C. Woolley, S.A. Lopez-Rivera, B.R. Pamplin, Sol. State Commun. 35 (1980) 573.
[9] R.G. Goodchild, O.H. Hughes, J.C. Woolley, Phys. Stat. Sol. (a) 68 (1981) 239.
[10] R.G. Goodchild, O.H. Hughes, S.A. Lopez-Rivera, J.C. Woolley, Can. J. Phys. 60 (1982) 1096.
[11] W.-T. Kim, Phys. Rev. B 44 (1991) 8667.
[12] V. Petrov, F. Noack, V. Badikov, G. Shevyrdyaeva, V. Panyutin, V. Chizhikov, Appl. Opt. 43 (2004) 4590.
[13] P.G. Schunemann, K.T. Zawilski, T.M. Pollak, J. Crystal Growth 287 (2006) 248.
[14] K. Mitin, A. Seryogin, V.V. Badikov, V.I. Chizhikov, V.L. Panyutin, G.S. Shevyrdyaeva, S. Sheina, "$AgGaGe_3Se_8$ nonlinear crystals," Photonics West, 24–29 Jan. 2004 (San Jose, CA, USA), Conference 5337: Nonlinear Frequency Generation and Conversion: Materials, Devices, and Applications III, paper [5337–32], Technical Summary Digest, p. 245.
[15] G.E. Davidyuk, I.D. Olekseyuk, G.P. Shavarova, G.P. Gorgut, Inorg. Mater. 41 (2005) 923. Transl. from Izv. Ross. Akad. Nauk: Neorganicheskie Materialy 41(2005) 1054.
[16] N.K. Trotsenko, private communication (1980–1981), unpublished.
[17] J.-J. Zondy, D. Touahri, O. Acef, J. Opt. Soc. Am. 14 (1997) 2481.
[18] J.-J. Zondy, Opt. Commun. 119 (1995) 320.
[19] D.N. Nikogosyan, Nonlinear Optical Crystals. A Complete Survey, Springer, 2005.
[20] A. Harasaki, K. Kato, Jpn. J. Appl. Phys. 36 (1997) 700.